Stem Cell Reports, Volume *12*

Supplemental Information

Sox10 Regulates Plasticity of Epithelial Progenitors toward Secretory Units of Exocrine Glands

Harleen K. Athwal, George Murphy III, Ellis Tibbs, Ashley Cornett, Emily Hill, Kenji Yeoh, Elsa Berenstein, Matthew P. Hoffman, and Isabelle M.A. Lombaert

SUPPLEMENTAL FIGURES AND DATA

Sox10 Regulates Plasticity of Epithelial Progenitors towards Secretory Units of Exocrine Glands

Harleen K. Athwal[1,2,#], George Murphy III[1,2,#], Ellis Tibbs[3,#], Ashley Cornett[1,2], Emily Hill[1,2], Kenji Yeoh[1,2], Elsa Berenstein[3], Matthew P. Hoffman[3], Isabelle M.A. Lombaert[1,2,3,*]

SUPPLEMENTAL FIGURE 1

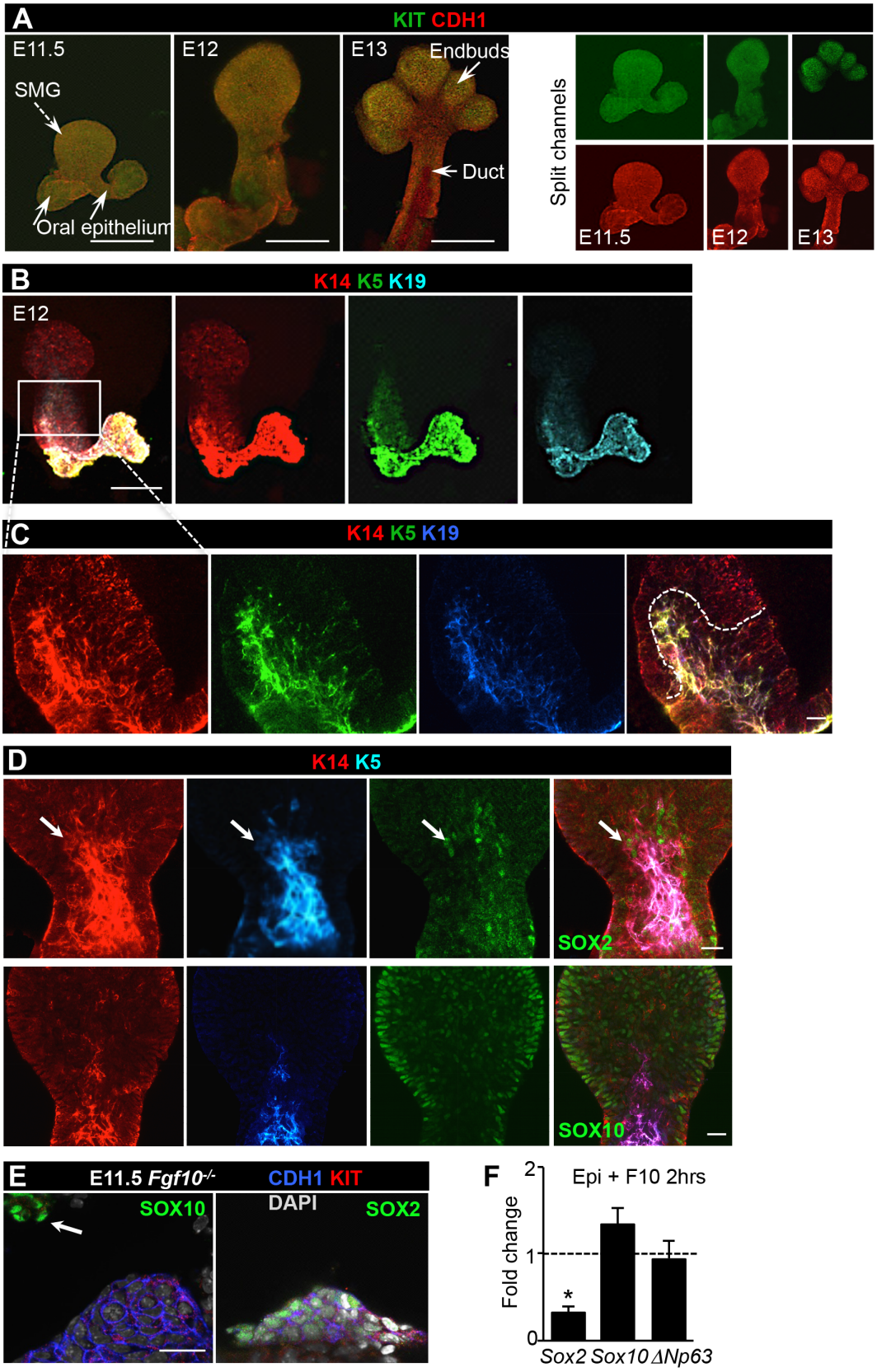

SUPPLEMENTAL FIGURE 2

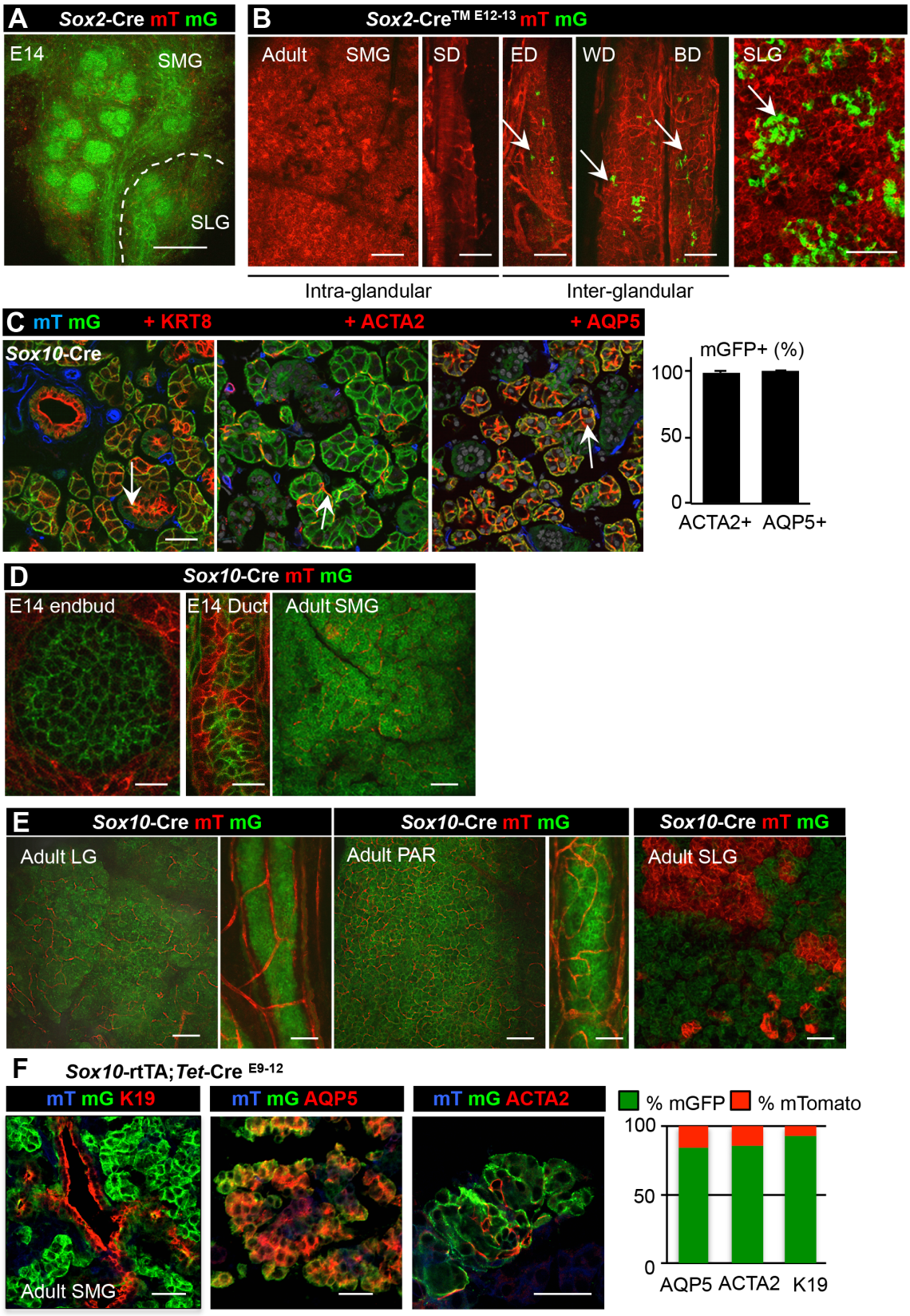

SUPPLEMENTAL FIGURE 3

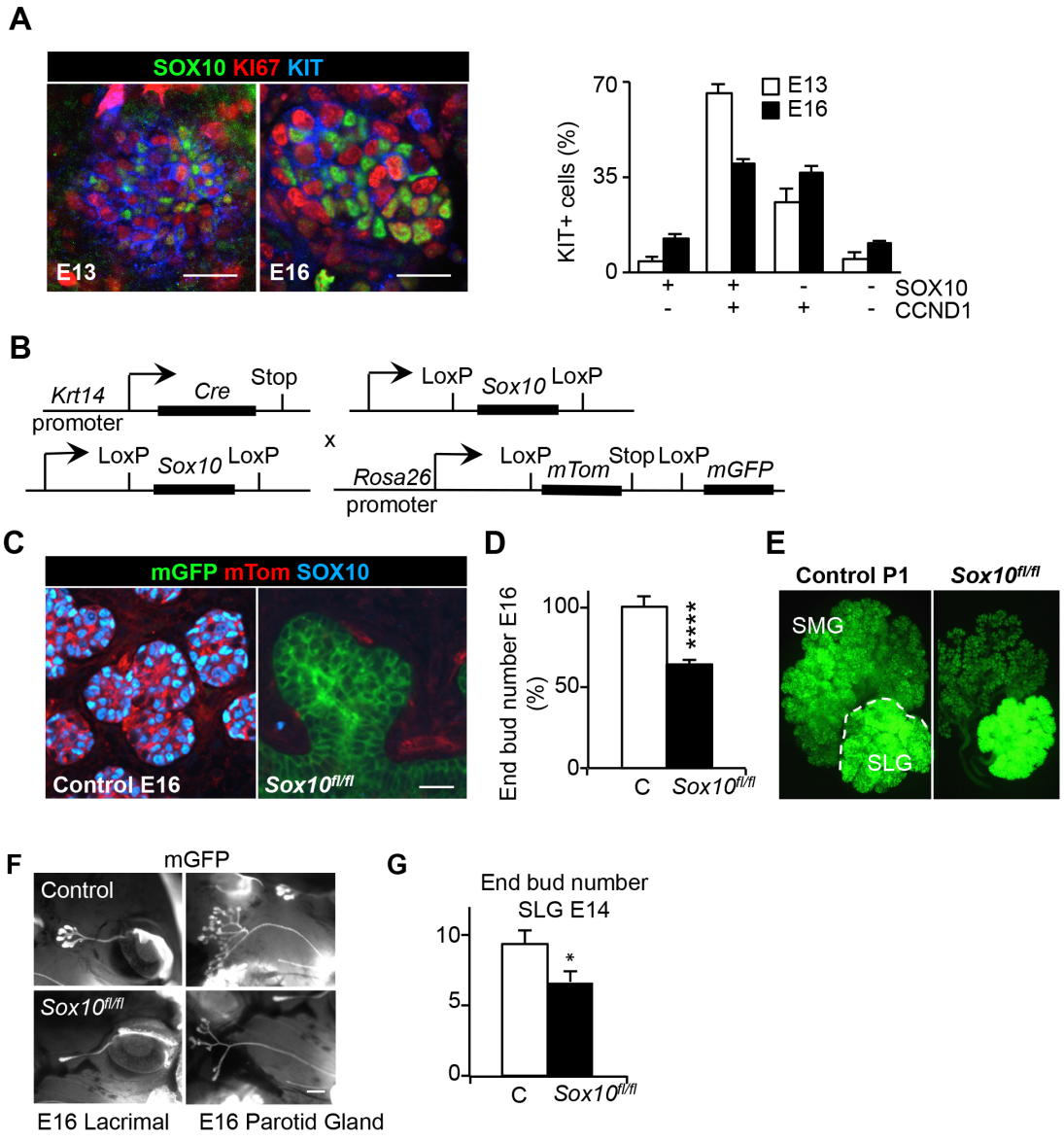

SUPPLEMENTAL FIGURE 4

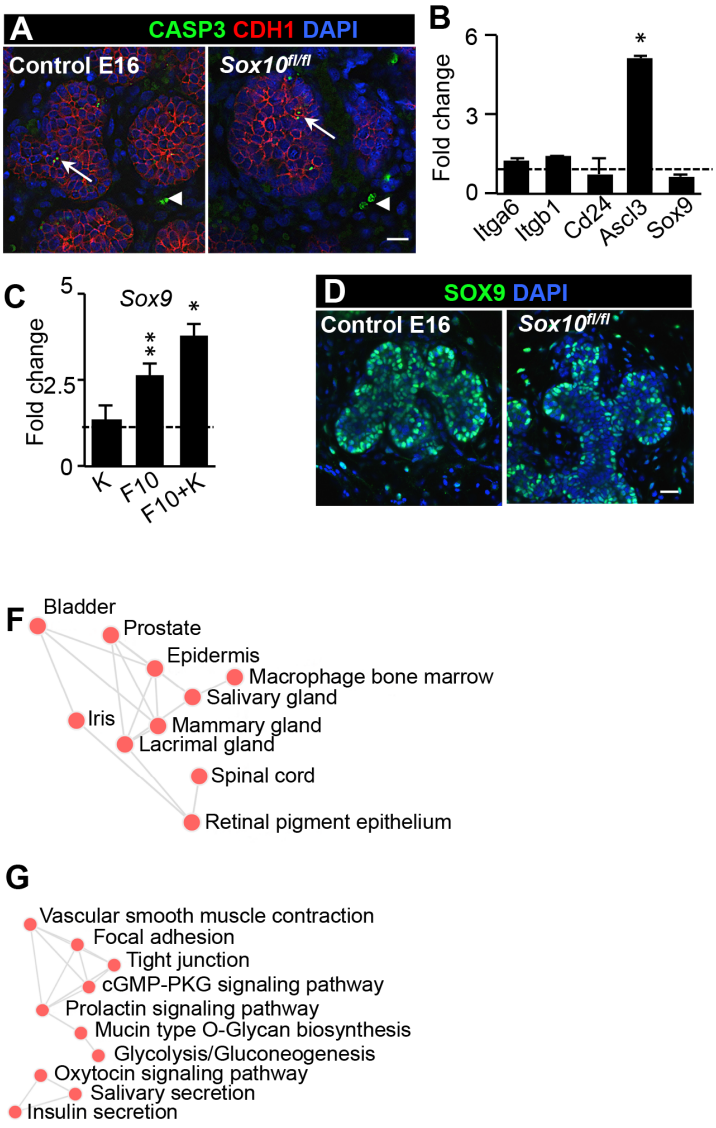

E

Gene	*- Log2* F.C.	*P*-value
Gyk	0.49	1.56E-05
Gm14584	0.49	7.96E-05
Cited4	0.49	1.54E-04
Lpo	0.49	1.62E-04
Abcc8	0.49	1.12E-04
Trpv6	0.48	5.30E-05
Tnfrsf11a	0.48	4.65E-05
Pgm5	0.48	3.55E-05
Cited1	0.48	2.17E-04
B3galt5	0.47	1.71E-06
Ceacam1	0.47	3.11E-05
Rap1gap	0.47	2.47E-04
Nrg2	0.47	1.99E-04
Gm23455	0.46	1.35E-05
Wwc1	0.46	5.03E-05
Nkx3-1	0.45	2.64E-04
Galnt7	0.45	7.37E-05
Bcar3	0.44	3.75E-05
Sntb1	0.44	6.01E-05
Ssfa2	0.43	3.02E-05
Gucy1b3	0.42	6.44E-06
Abtb2	0.40	9.90E-05
Btnl9	0.40	2.59E-04
Gm24357	0.39	2.63E-04
Dll1	0.37	1.88E-04
Esp8	0.37	2.19E-04
Msrb3	0.37	7.89E-05
Eno1	0.37	5.87E-05
Smyd5	0.36	1.73E-04
Papl	0.35	5.93E-05
Mylk	0.34	1.12E-05
Smr3a	0.32	7.41E-05
Synj2	0.30	1.73E-04
Ntn1	0.26	2.61E-04

SUPPLEMENTAL FIGURE 5

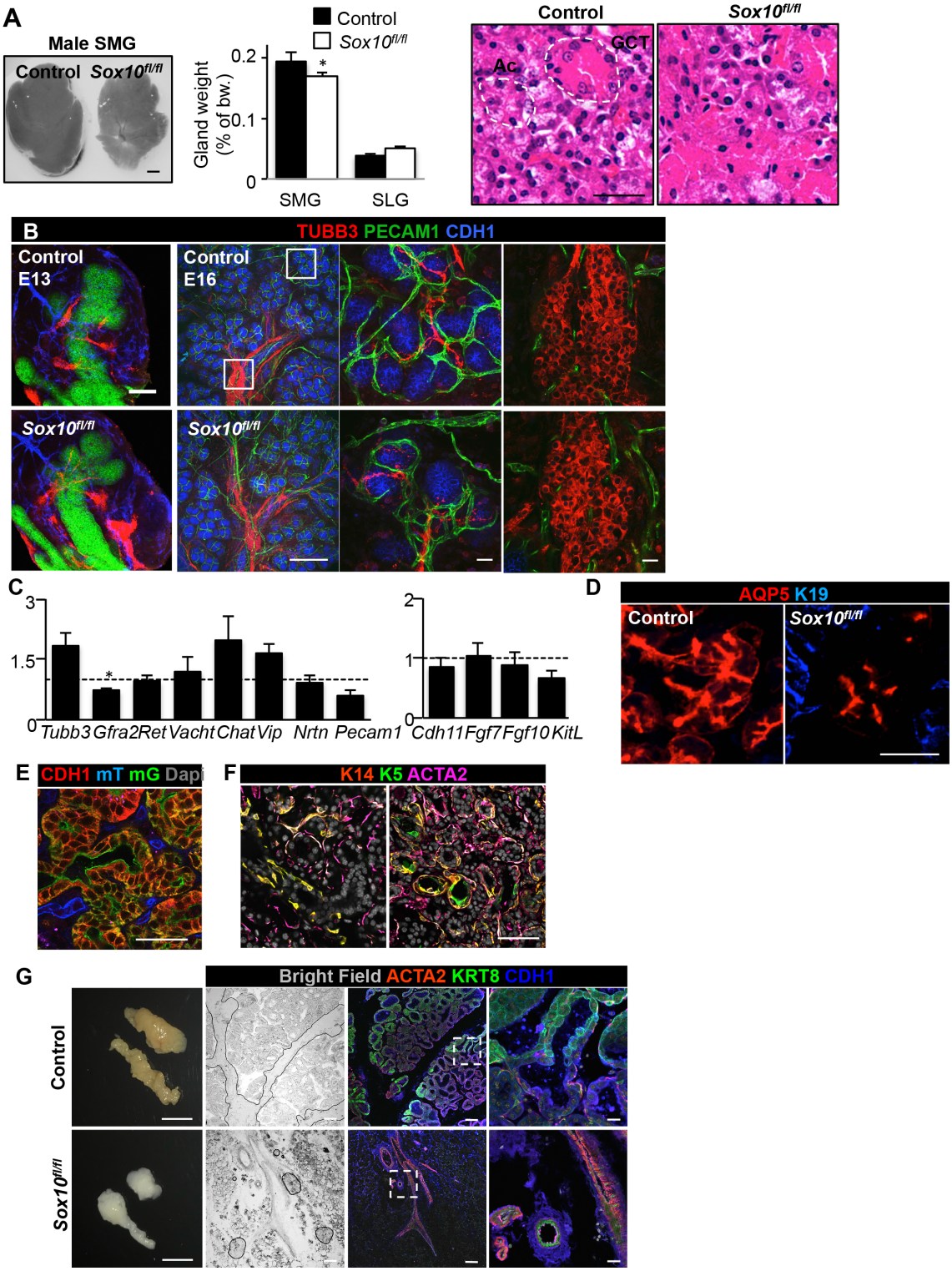

SUPPLEMENTAL FIGURE 6

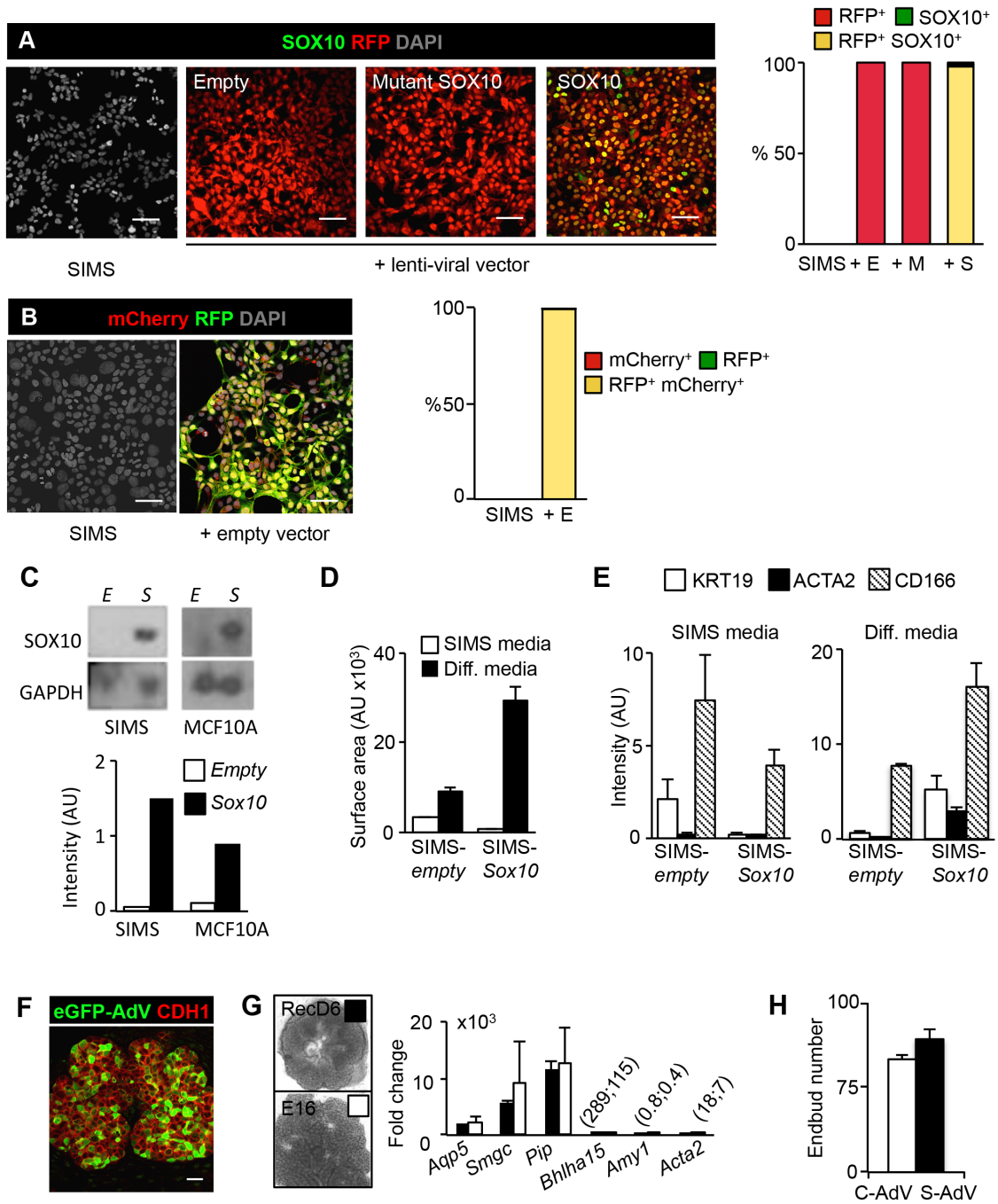

SUPPLEMENTAL FIGURE LEGENDS

FIGURE S1. Expression patterns of KIT and Keratins in epithelia of developing exocrine glands, Related to Figure 1.

(A) Confocal images (overlay and split images) of isolated epithelia (E11.5-13) stained for KIT and E-cadherin (CDH1). Arrows indicate oral epithelium (E11.5), main duct and endbuds (E13), and salivary submandibular gland (SMG, dotted arrow). Scale bar, 100 μm.

(B-C) Maximum projection and high power 2μm confocal image of isolated E12 SMG epithelia with attached oral epithelium stained for K14, K5, and K19. Dotted line indicates border of $K14^{+}K5^{+}K19^{+}$ and $K14^{+}$ cells. Scale bar, 100 μm and 20 μm.

(D) Confocal images of E11.5 isolated SMG epithelia stained for SOX10, SOX2, K5 and/or K14. Arrows show $K14^{+}K5^{+}$ cells co-expressing SOX2. Scale bar, 20 μm.

(E) *Fgf10*$^{-/-}$ E11.5 isolated oral epithelia, stained for CDH1, KIT, SOX10 or SOX2, and DAPI. Arrow indicates non-epithelial neuronal $SOX10^{+}$ cell. Scale bar, 20 μm.

(F) Fold change in gene expression of *Sox2*, *Sox10* and *DNp63* in isolated E13 epithelia (epi) stimulated with FGF10 (F10, 100ng/mL) for 2 hours. Data was normalized to *Rps29* and unstimulated epithelia (dotted line), Mean±SEM, N=3, Unpaired t-test. *, P<0.05.

FIGURE S2. Contribution of early *Sox2* or *Sox10* cells to exocrine glands, Related to Figure 2.

Multiple transgenic mice designed for lineage tracing were crossed with *Rosa26*-mTmG mice to acquire tissue for confocal images. Images show $mGFP^{+}$ cells (mG) as green and

mTomato^{+} cells (mT) as red, with the exception of (C) and (F) where mT is pseudo-colored in blue.

(A) Confocal imaging of E14 SMG and SLG from *Sox2*-Cre mice. Scale bar, 100 μm.

(B) *Sox2*-Cre^{TM} mice crossed with *Rosa26*-mTmG mice were induced at E12-13 and adult SMG and SLG were analyzed by confocal microscopy. Intra-glandular striated ducts (SD), and inter-glandular excretory (ED), Wharton's and Barthon's ducts (WD and BD) are shown. Arrows indicate mG^{+} cells. Scale bar, 20 μm.

(C) Confocal imaging of adult SMG sections from *Sox10*-Cre mice, co-stained for KRT8, ACTA2 or AQP5. Arrows represent mGFP^{+} cells co-expressing KRT8, ACTA2 or AQP5. Scale bar, 20 μm. Graph represents quantification (%) of all ACTA2^{+} and AQP5^{+} cells expressing mGFP. Mean±SEM, N>3 with scoring of more than 3 areas with 3 slides per SMG.

(D) Lineage tracing of *Sox10*-Cre mice at E14 (endbuds and main duct region) and adult SMGs were analyzed by confocal microscopy. Scale bar, 20 and 100 μm.

(E) Adult *Sox10*-Cre lacrimal (LG), parotid (PAR), sublingual glands (SLG) and designated main duct were analyzed by confocal microscopy. Scale bar, 20 and 100 μm.

(F) Adult SMG cryosections stained for K19, AQP5 and ACTA2 were analyzed by confocal microscopy. Glands derived from *Sox10*-rtTA;*Tet*-Cre mice were crossed with *Rosa26*-mTmG mice and induced with doxycycline from E9-12. Scale bar, 20 μm. Graph represents quantification of AQP5+ (84.7±0.1%), ACTA2+ (85.5±0.1%) and K19+ (90.9±0.1%) cells co-expressing mGFP or mTomato. N>3 with scoring of more than 3 areas with 3 slides per SMG.

FIGURE S3. Loss of *Sox10* impacts overall exocrine gland development, Related to Figure 3.

(A) Confocal pictures of KIT, SOX10 and KI67 co-staining in E13 and E16 SMG endbuds. Scale bar, 20 μm. Graph represents KIT^+ subpopulations counted on multiple sections through endbuds at each time-point. *N*>3, Mean ± SEM.

(B) Graphical outline demonstrating Cre-*flox* system used with the *Krt14* promoter, $Sox10^{flox/flox}$ and/or *Rosa26*-mTomato-mGFP (mTmG) mice.

(C) Confocal image of E16 control (*Rosa26*-mTmG) and $Sox10^{fl/fl}$ SMG endbuds, stained for SOX10. Scale bar, 20 μm.

(D) Quantification of endbud number in E16 SMGs from control and $Sox10^{fl/fl}$ mice. Data was normalized to control (C), Mean±SEM, *N*>3, Unpaired *t*-test. ****, *P*<0.0001. Control (100.0±6.3% endbuds); $Sox10^{fl/fl}$ (64.8±2.8% endbuds).

(E) Fluorescent image of mGFP expression in P1 SMG and SLG of $SOX10^{fl/+}$ control (*K14*-Cre*;Rosa26*-mTmG) and $Sox10^{fl/fl}$ mice. Scale bar, 500 μm.

(F) Fluorescent images of mGFP expression, pseudo-colored in black and white, of lacrimal gland and parotid gland of E16 control and $Sox10^{fl/fl}$ mice. Scale bar, 500 μm.

(G) Quantification of endbud number in E14 SLGs from control and $Sox10^{fl/fl}$ mice. Mean ± SEM, *N*>3, Unpaired *t*-test. *, *P*<0.05. Control (9.3±1.2) vs $Sox10^{fl/fl}$ (6.7±0.7).

Figure S4. Analysis of E16 $Sox10^{fl/fl}$ SMGs and changes in cell plasticity by forced overexpression of *Sox10*, Related to Figure 4.

(A) Confocal image representing distal area of E16 control or $Sox10^{fl/fl}$ SMGs. Tissue was stained for cleaved-caspase 3 (CASP3), E-cadherin (CDH1) and nuclei (DAPI). Arrows

indicate cell apoptosis in epithelia, arrowheads indicate cell death in surrounding environment. Scale bar, 20 μm.

(B) Fold changes in expression of progenitor-related markers in E16 *Sox10*$^{fl/fl}$ SMGs. Data was normalized to *Rps29* and control (dotted line). Mean±SEM, *N*>3, Multiple comparison *t*-test. *, *P*<0.05.

(C) Fold change in expression of *Sox9* in isolated E13 epithelia after a 3 hour stimulation with ligands KIT Ligand (K, 100ng/mL) and/or FGF10 (F10, 100ng/mL) to activate KIT/FGFR2b signaling. Data was normalized to *Rps29* and unstimulated epithelia (dotted line). Mean±SEM, *N*>3, Unpaired *t*-test. **, *P*<0.01; *, *P*<0.05.

(D) SMGs from E16 control and *Sox10*$^{fl/fl}$ mice were stained for SOX9 and DAPI, and analyzed by confocal microscopy. Scale bar, 20 μm.

(E) Continuing list of downregulated genes in E16 *Sox10*$^{fl/fl}$ SMGs versus control from Figure 4. The list was generated after bioinformatical analysis of next-generation sequencing data and cut-off at *Log2* fold change *(F.C)* of -0.25.

(F-G) Bioinformatic analysis of next-generation sequence performed on E16 control and *Sox10*$^{fl/fl}$ SMGs. Data was used as input for computing enrichment with existing lists of mouse gene atlas (F), and KEGG pathways (G).

Figure S5. Cellular changes in developing and adult *Sox10*$^{fl/fl}$ SMGs, Related to Figure 5.

(A) Bright field images of adult male SMGs from control and *Sox10*$^{fl/fl}$ mice. Scale bar, 1 mm. Graphs represent weight of SMGs as a percentage of body weight (bw.). Male SMG (control: 0.19±0.01%, *Sox10*$^{fl/fl}$: 0.16±0.01%). Male SLG (control: 0.03±0.01%, *Sox10*$^{fl/fl}$:

0.04±0.01%). Mean±SEM, *N*>3, Unpaired *t*-test. *, *P*<0.05. Hematoxylin-Eosin staining of SMGs of control and *Sox10*$^{fl/fl}$ mice. Scale bar, 25 μm. Acini (Ac) and granulated convoluted tubules (GCT), which are predominantly present in male glands, are outlined.

(B) Confocal imaging of E13 and E16 control and *Sox10*$^{fl/fl}$ SMGs, co-stained for TUBB3, PECAM1 and E-cadherin (CDH1). White boxes around the distal endbuds or ganglia are enlarged. Scale bar, 100 and 20 μm.

(C) qPCR analysis of environmental-related genes of E16 control and *Sox10*$^{fl/fl}$ SMGs. Data was normalized to *Rps29* and control (dotted line). Mean±SEM, *N*>3, Unpaired *t*-test. *, *P*<0.05.

(D) High power confocal image of AQP5 protein expression in epithelial cells from E16 control and *Sox10*$^{fl/fl}$ SMGs. Scale bar, 20 μm.

(E) Confocal image of adult SMG from the *Krt14*-Cre;*Sox10*$^{flox/flox}$*;Rosa26*-mTmG mouse. Tissue was co-stained for E-cadherin (CDH1). mTomato was pseudo-colored in blue. Scale bar, 20 μm.

(F) Outline of myoepithelial cells, expressing ACTA2, K14 and K5 in E16 control and *Sox10*$^{fl/fl}$ SMGs. Scale bar, 20 μm. Yellow represents overlap of K14 and K5 only in ducts.

(G) Bright field pictures of mammary glands (MMGs) from lactating control and *Krt14*-Cre;*Sox10*$^{flox/flox}$ mice. Scale bar, 0.5 cm (left). Staining of ACTA2, KRT8 and E-cadherin (CDH1) on MMG sections from control and *Krt14*-Cre;*Sox10*$^{flox/flox}$ mice. In control MMG, myoepithelial cells are ACTA2^{+}. Alveolar cells are KRT8^{-}CDH1^{+}. Ductal cells are KRT8^{+}CDH1^{+}. Right images are higher power from insets. Scale bar, 100 μm (low power) and 20 μm (high power).

Figure S6. Cellular changes in developing and adult *Sox10*$^{fl/fl}$ SMGs, Related to Figure 6.

(A) An adult duct cell line was non-transduced or transduced with empty lenti-viral vectors or with vectors containing mutant or wild-type *Sox10*. After transduction, cells were stained for DAPI, SOX10 and mCherry (RFP). Graph depicts quantification (%) of transduced cells expressing RFP and/or SOX10. Scale bar, 50 μm.

(B) Cells were non-transduced or transduced with empty lenti-viral vector, and stained for RFP (pseudo-colored in green) and DAPI. Graph shows quantification of the number of cells expressing mCherry and/or RFP. Scale bar, 50 μm.

(C) Western blot analysis for SOX10 and GAPDH on SIMS or MCF10A cells with *empty* lenti-viral vectors (*E*, *Empty*) or vectors containing *Sox10* (*S*, *Sox10*). Graph depicts semi-quantified analysis of SOX10 expression intensity in each cell type from representative blot. Data was normalized to GAPDH, and depicted in arbitrary units (AU).

(D) Quantification of surface area (arbitrary units) of organoids created by SIMS-*empty* or SIMS-*Sox10* cells by D7 in SIMS or differentiation media. Mean±SEM, $N>3$.

(E) Quantification of fluorescence intensity (arbitrary units) of KRT19, ACTA2, or CD166 expression on SIMS-*empty* or SIMS-*Sox10* cells in SIMS or differentiation media. Mean±SEM, $N=3$.

(F) Primary fetal E13 isolated epithelia was transfected with *eGFP*-AdV MOI 50, then recombined with mesenchyme and ganglia, and analyzed after 4 days for transfection efficiency. Tissue was stained for eGFP and E-cadherin (CDH1). Scale bar, 10 μm.

(G) Bright field picture of recombined SMG cultured for 6 days (rec D6) or E16 in vivo SMG. Both tissues were compared for gene expression related to myoepithelial, intercalated duct and acinar markers. Data was normalized to *Rps29*. Mean±SEM, $N>3$.

(H) Quantification of endbud number in recombined $Sox10^{fl/fl}$ SMGs transduced with *eGFP*-AdV (C-AdV) or *Sox10*-AdV (S-AdV). Mean±SEM, $N>3$.

SUPPLEMENTARY MATERIALS AND METHODS

Animal care and use

All mice used in the study were housed and bred in Specific Pathogen Free (SPF) rooms located in the AAALAC-accredited University of Michigan vivarium at the North Campus Research Center or at NIDCR at NIH. For timed-matings the morning of plug detection was considered day 0.5 post-coitum. Genotyping of mice was performed on tail biopsies by PCR and agarose gel electrophoresis using specific primers. *Krt14*-Cre mice, as used in (Lombaert et al., 2013), were crossed with Gt(Rosa)26Sor $^{tm4(ACTB-tdTomato,-EGFP)Luo}$ (Jackson Laboratory) and/or *Sox10*$^{flox/flox}$ mice that were obtained from Dr. M. Wegner (Finzsch et al., 2010). Multiple mice were gifted from various sources: *Fgf10*$^{-/-}$ from Dr. I. Nobuyuki (Kyoto University), *Sox2*-Cre from Dr. Y. Yamada (NIH), *Sox2*-Cre^{TM} from Dr. K. Hochedlinger (Harvard, MGH) and *Sox10*-rtTA (Dr. M. Wegner). Also mice were purchased: *Sox10*-Cre, *Tet*-Cre and timed-pregnant ICR female mice (Harlan, IN). Both female and male mice were evaluated at adult stages, which was considered 6 weeks old and beyond.

Ex vivo organ culture, recombination assays and adenovirus transduction

Adenovirus transduction was performed by transfecting isolated epithelia for one hour with *Sox10*-AdV (Vector Biolabs, AdV-272873) or eGFP-AdV (Vector Biolabs, 1060) before recombination. The transfection efficiency of the AdV in fetal E13 epithelia was found to be 74±8%.

Quantitative PCR

cDNA was generated from DNAse-free RNA, amplified and gene expression was normalized to house-keeping gene, *Rps29*. Experiments were run in technical triplicates with at a minimum of three biological samples.

Immunohistochemistry/fluorescence

Fluorescently labeled secondary antibodies and DAPI were used to visualize the proteins and nuclei, and Zeiss Confocal microscopy was used to analyze the images.

Adult tissue was fixed in 4% formaldehyde and processed for OCT cryosections. Tissue was labeled with primary and secondary antibodies and imaged, similar to embryonic tissue. Adult tissue was also fixed in 4% formaldehyde and processed for paraffin embedding. Paraffin sections were stained for hematoxylin-eosin staining and analyzed by bright field microscopy. More info on the antibodies used can be found in Supplementary Data.

Primary antibodies used: ACTA2 (Sigma, A2547), TUBB3 (RnD Systems, MAB1195), AQP5 (Alomone, AQP-005), KRT7 (Abcam, Ab9021), KRT8 (DSHB, Troma I), GFP (Abcam, Ab13970), SMGc (Antibody Online, ABIN1104377), BHLHA15 (Abcam, ab187978), SOX10 (Santa Cruz, sc-17342), KIT (RnD systems, MAB1195), CDH1 (Cell Signaling, 3195S), KRT5 (Covance PRB-160P), KRT14 (Covance, PRB-155P), KRT19 (DSHB, TROMA III), PECAM1 (BD Biosciences, 553708), SOX2 (Santa Cruz, sc-17320), CCDN1 (Abcam, ab16663), cleaved CASPASE3 (Cell Signaling, 9661), SOX9 (Chemicon, Ab5535), and CD166 (Santa Cruz, sc-74558).

ImageJ was used to quantify endbud number using bright field pictures, or GFP intensity in designated field using fluorescent images, or for quantification of co-expressed mGFP in acinar (AQP5), myoepithelial (ACTA2) and ductal cells (KRT19).

Western blot analysis and coomassie staining

Protein from saliva was resolved on Bis-Tris gels, stained for coomassie (10mg protein loaded per lane) or transferred to membranes, and probed with antibodies for MUC10 (ProSci, 42-311) or alpha-amylase (Sigma, A8273) (20mg protein loaded per lane). West Dura reagent was used for visualization. A more detailed western protocol is described in (Lombaert et al., 2013).

RNA-sequencing and bioinformatics analysis

For each RNA sample, cDNA libraries were made using the T
rueSeq RNA Sample Preparation kit (Illumina). 50bp single-ends were sequenced on the Illumina HiSeq 2500. Quality control was performed on the raw sequencing reads using FASTQC. Consequently, reads were mapped to the Mus musculus genome (Build mm9) with TopHat2 using Bowtie2. PCA analysis was used to outline the experimental groups, and bioinformatics analysis was performed to provide a Log2 fold in expressions.

Lentiviral overexpression in MCF10A and SIMS cells

A constitutively active lentiviral backbone, pLVX-EF1alpha-IRES-mCherry, was utilized for the overexpression in which we cloned mouse *Sox10* that shares 99% homology with the human *Sox10.* The empty vector or mutated inactive version of *Sox10* that was

truncated for first 150bps was used as control, which does not form SOX10 protein. Each cell type was transfected for control and *Sox10* virus in a 24 well plate. The MOI was 20.1. Cells were passaged to a 10 cm plate before flow sorting. Cells with empty or *Sox10* overexpressed vectors were sorted against mCherry to attain a homogeneous population. Cells were maintained in a T75 flask, and each passage was used for qPCR analysis.

Alternatively, a LentiX Tet-ON 3G (Takarabio) doxycycline inducible system was utilized to induce *Sox10* in SIMS cells. SIMS cells were first infected with virus particles carrying the Tet-ON 3G backbone with a neomycin selection cassette. A stable SIMS-Tet cell line, with MOI 60.35, was hereby generated. *Sox10* was inserted in a puromycin selectable pLVX-TRE3G backbone. Stable SIMS-Tet cells were infected with MOI 64.9, and selected with puromycin and neomycin for a stable inducible cell line. Control cell line, pLVX-Empty, was generated using virus carrying the pLVX-TRE3G backbone, which was infected with MOI 62.9 to SIMS-Tet cells. The cell lines were induced using 1μg/mL concentration of doxycycline for experimental purposes. Upon daily doxycycline activation, the Tet-ON-*Sox10* cells showed similar results to constitutive expression of the SIMS-*Sox10*-mCherry cells.

3D culture of SIMS cells

Ten thousand empty or SOX10-overexpressing single SIMS cells (in 25μL) were plated in 3D Matrigel GFR (BD Biosciences)/rat collagen type I (60/40), and allowed to solidify for 20 minutes at 37C. Cells were grown either in SIMS media (Laoide et al., 1996) or differentiation-inducing media. The latter consists of SIMS media with Glutamax (1x),

ITS (1x), N2 supplement (1x), EGF (20ng/mL), Fgf2 (20ng/mL), Dexamethasone (1uM), Triiodothyronine (2nM), Retinoic acid (0.1uM), Hydrocortisone (0.4ug/mL), Cholera toxin (8.5ng/mL), and Calcium (0.8mM). In some occasions, 1μg/mL doxycycline was added and media was replaced every 2 days. Outgrowth of cells was observed at day 7 (D7). The surface area of growth was calculated, and cell containing 3D gels were processed for protein staining. *N*=3 biological samples for each condition.
Surface area or fluorescence intensity was calculated in Image J and represented in arbitrary units.

Statistical Analysis and Data Availability

Statistical significance was determined by *p*-values of less than 0.05, with all experiments having at least 3 biological replicates. Unpaired *t*-test was used when comparing two groups. Determining significance of individual variables within a group of variables tested under different conditions, a multiple comparison *t*-test was used. Graphs show Mean±SEM for each group. $P<0.05$ was considered statistically significant.
RNASeq data is available on the Gene Expression Omnibus (GEO) website (GSE123341).

REFERENCES

Finzsch, M., Schreiner, S., Kichko, T., Reeh, P., Tamm, E.R., Bosl, M.R., Meijer, D., and Wegner, M. (2010). Sox10 is required for Schwann cell identity and progression beyond the immature Schwann cell stage. J Cell Biol *189*, 701-712.

Laoide, B.M., Courty, Y., Gastinne, I., Thibaut, C., Kellermann, O., and Rougeon, F. (1996). Immortalised mouse submandibular epithelial cell lines retain polarised structural and functional properties. J Cell Sci *109 (Pt 12)*, 2789-2800.

Lombaert, I.M., Abrams, S.R., Li, L., Eswarakumar, V.P., Sethi, A.J., Witt, R.L., and Hoffman, M.P. (2013). Combined KIT and FGFR2b signaling regulates epithelial progenitor expansion during organogenesis. Stem Cell Reports *1*, 604-619.